



## Supporting Online Material for

### **A Melanocortin 1 Receptor Allele Suggests Varying Pigmentation Among Neanderthals**

Carles Lalueza-Fox,\* Holger Römpler, David Caramelli, Claudia Stäubert, Giulio Catalano, David Hughes, Nadin Rohland, Elena Pilli, Laura Longo, Silvana Condemi, Marco de la Rasilla, Javier Fortea, Antonio Rosas, Mark Stoneking, Torsten Schöneberg, Jaume Bertranpetit, Michael Hofreiter\*

\*To whom correspondence should be addressed. E-mail: clalueza@ub.edu (C.L.-F.); hofreite@eva.mpg.de (M.H.)

Published 25 October 2007 on *Science Express*  
DOI: 10.1126/science.1147417

#### **This PDF file includes:**

Materials and Methods  
Figs. S1 to S5  
Tables S1 to S4  
References

## Supplementary online material

### Materials and methods

**Description of Neanderthal sites and specimens** The Monti Lessini sample is comprised of several skull fragments with Neanderthal diagnostic features from the Riparo Mezzena site, near Verona (North of Italy). These fossils include an incomplete jaw, represented by the symphyseal region and a section of the mandibular corpus, as well as 13 fragments, two of which belong to the post-cranial skeleton, excavated in the Riparo Mezzena site (*S1*). The cranial fragments belong to the frontal, occipital and parietal bones. The thickness of all cranial fragments falls outside the range of variation for modern Europeans and lies within the upper range of variation for Neanderthals (*S2*). In view of their state of preservation and the thickness of the bones, these fossil remains may have belonged to a single adult individual, although it is not possible to fit them together. One of the small fragments of the parietal bone was used for DNA extraction. The Monti Lessini sample has been dated stratigraphically to ~50,000 years ago.

El Sidrón is a deep and narrow karstic (an area of irregular limestone subject to erosion) system close to the Cantabrian mountain range in Asturias (north of Spain), where at least nine Neanderthals accumulated after the collapse of a sinkhole (doline) in the surface (*S3*). The main gallery is a tunnel about 600 m of length that runs from West to East, showing some blind transversal galleries in its central section (*S4*). The fossil site in one of these galleries, named “Galeria del Osario”, comprises a small area of about 6 m<sup>2</sup> and is situated 220 m from the main entrance of the system. Sediments accumulated at the Galeria del Osario constitute a deposit mostly composed of clay, so far prospected to about 227 cm in depth (*S3*). More than one thousand Neanderthal skeletal fragments have been retrieved since the initial, accidental discovery in 1994. The bones have been radiocarbon dated to ~43,000 years (*S3*).

**Amino acid content and racemisation** Stereoisomers of aspartic acid, glutamic acid, and alanine of the fossils were determined and amino acid analyses were performed as previously described (*S5*, *S6*). Both samples showed low racemization (aspartic acid D/L ratios of 0.02 and 0.074 for El Sidrón and Monti Lessini, respectively) and high overall amino acid content (37,188 p.p.m. for Monti Lessini and 126,250 p.p.m. for El Sidrón) (*S5*, *S6*).

**Ancient DNA extraction** For Monti Lessini, bone powder was removed by drilling into one cranial fragment. 1.5 g were used for DNA extraction at the Florence ancient DNA laboratory, while DNA was extracted from 0.5 g at the Barcelona ancient DNA laboratory. For El Sidrón 1252, one sample of 0.5 g was used for DNA extraction at the Barcelona laboratory. Extractions were performed as described (*S7*). In short, powdered samples were decalcified, incubated with proteinase K in lysis buffer and then phenol:chloroform extracted followed by silica purification. Ten milliliters of EDTA (pH 8; 0.5 M) were added to the powder and incubated at 37°C for 12 h. After centrifugation, the liquid phase was discarded and the remaining pellet was incubated at 50°C for 12 h in 10 mL lysis buffer (0.5% SDS, 50 mM TRIS, and 1 mg/mL of proteinase K in H<sub>2</sub>O). Next, the samples were extracted successively with phenol, phenol-chloroform and chloroform-isoamylic alcohol. The extract was concentrated to a final volume of 150 µl with centricon filters (Millipore, Billerica, MA, USA) with a 30,000 Dalton molecular cut-off. Finally, the DNA was purified by binding to silica and eluted in a final volume of 50 µl double distilled water.

In Leipzig the previously extracted bone pellet from the El Sidrón specimen [used for sequences replication (*S6*)] was re-extracted with a modified silica extraction method that uses only EDTA and proteinase K as extraction buffer (*S8*). In addition, a 1:5 dilution of the Monti Lessini extract used in Barcelona was provided by C. L.-F. All ancient DNA experiments were conducted in dedicated ancient DNA laboratories following the appropriate precautions for work with Neanderthal DNA (*S9*). During all experiments, extraction and PCR blank controls were completed alongside the Neanderthal samples to monitor for possible contamination.

**Ancient DNA amplification** In Barcelona and Florence the following PCR conditions were used: 2 units AmpliTaq Gold DNA Polymerase (ABI, Foster City, CA, USA), 1 x GeneAmp PCR (ABI, Foster City, CA, USA), 4 mM MgCl<sub>2</sub>, 500 μM for each dNTP and 1.50 μM of each primer in a final volume of 20 μl. Amplification conditions in Florence were 10 min activation at 94°C, followed by 60 cycles of 94°C for 20 s, 50° for 30 s, and 72°C for 30 s. In Barcelona, a two-step PCR protocol (*I0*) was used. Primary amplification consisted of a 10 min activation step at 94°C, followed by 27 cycles at 94°C for 20 s, 50°-55°C (primer dependent) for 30 s, and 72°C for 30 s. In the second PCR step, conditions were as described for the first step except that the primer concentration was increased to 1.5 μM for each primer and that 33 cycles were performed. Five μl of the silica purified DNA extracts were used as template in both laboratories. Primers used had the following sequences (5'→3'): L846-TCTTCAAGAACTTCAACCTC, H936- 13 TCACCAGGAGCATGTCAGC, L884-TGCAATGCCATCATCGACCC, L906- TCATCTACGCCTTCCACAGC and H924-ATGTCAGCACCTCCTTGAGC.

In Leipzig 5 μl of Monti Lessini extract from Barcelona (1:5 dilution) and 5 μl of El Sidrón re-extract were used in PCRs performed under the same conditions as in Florence, except for newly designed primers (5'→3'): L911-CGCCTTCCACAGCCAGGA and H924a-CAYGTCAGCACCTCCTTGAGC, 250 μM of each dNTP, 0.25 μM of each primer and an annealing temperature of 60°C. In addition, we attempted to obtain the complete coding sequence of *mc1r* via multiplex PCR [setup as described (*S10*)]. As template, we used 5 μl of extract (pure, 1:3 or 1:9 dilution) obtained by re-extracting (*S8*) a previously extracted bone pellet from El Sidrón, and 5 μl of dilutions of Monti Lessini extract prepared in Barcelona in a multiplex PCR. Due to the dilution, DNA concentrations in the PCR were only 10% to 20% compared to those obtained in Barcelona. Only a few of the primer pairs yielded very short PCR products, and contamination was observed in some of the controls. Furthermore, no undiluted extract from Monti Lessini and no additional bone fragments from either specimen were available. Therefore, we had to abandon our attempt to obtain the complete *mc1r* sequence.

Altogether, we observed the A to G change for the Monti Lessini sample in 2/2 attempts in Barcelona, 1/1 in Florence and in 2/3 attempts in Leipzig (Figure S1), and for El Sidrón in 4/4 attempts in Barcelona and in 0/2 in Leipzig. Although no DNA damage is known for ancient DNA that would cause an A to G change (*S11*, *S12*), we tried to calculate the probability that the observed pattern could be caused by an unknown damage occurring at the same frequency as cytosine deamination (~2%), the most common type of damage in ancient DNA. However, as we do not know from how many template molecules each reaction started and moreover, the PCRs may have been affected by contamination with modern human DNA to varying degrees, we assumed that all clones showing the G at position 919 in an individual PCR go back to the same template molecule. As we amplified nuclear DNA, this is probably a reasonable assumption. Therefore we used a binomial distribution to calculate the

probability to obtain an A to G change due to damage affecting 2% of all As in the sequence. We did the calculation both for the combined data set (9/12 attempts successful), and each sample alone (4/6 for El Sidrón and 5/5 for Monti Lessini). Investigated individually the probability for Monti Lessini is  $\sim 2 \times 10^{-8}$ , whereas it is  $\sim 0.015\%$  for El Sidrón alone. For the combined data set, the probability is  $\sim 10^{-13}$ .

**Amplicon separation, purification, cloning and sequencing** The following steps were completed according to the same protocols in all three laboratories (Barcelona, Florence and Leipzig): After separation and visualization of PCR products on 2% agarose gels (*S13*), amplification products of the correct size were isolated from the gel and purified using a silica based method. No spurious DNA bands were observed, although due to the low amount of endogenous target DNA, some amplifications yielded no products at all. Purified PCR products were cloned with the TOPO TA Cloning kit (Invitrogen, Karlsruhe, Germany), following the manufacturer's instructions. Colonies were subjected to PCR with M13 universal primers; inserts of the right size were sequenced with Applied BioSystems DNA sequencers (ABI, Foster City, CA, USA). An overview for all amplifications from both Neanderthal samples and the percentage of clones carrying G at position 919 is shown in Table S1. Clones from all amplifications are depicted in Figure S1.

**CEPH Panel genotyping** The entire CEPH Human Diversity Panel, consisting of 1,051 individuals from 51 populations (*S14*) was genotyped for the A to G substitution at nucleotide position 919 (from the reference open reading frame of the *mc1r* NM\_002386). Usable results were obtained for 985 individuals.

Genotyping was performed with single base pair extension (SBE) and detected by matrix assisted laser desorption/ionization time of flight (MALDI-TOF) mass spectrometry. PCR reactions were performed with 35 cycles, an annealing temperature of 55°C, 20 ng of template DNA, 1 x PCR buffer (ABI, Foster City, CA, USA), 200  $\mu$ M dNTPs (Amersham, Uppsala, Sweden), 100 nM of each primer (5'→3') CATCTCACACTCATCGTCCTCT and CACGTCAGCACCTCCTTGAG, and 1.25 units of AmpliTaq Gold DNA Polymerase (ABI, Foster City, CA, USA). Eight microliters of each amplified product were subsequently digested with 0.3 units of Shrimp alkaline phosphatase (Amersham, Buckinghamshire, England) and 0.2 units Exonuclease I (ExoI) (NEB, Ipswich, MA, USA) at 37°C for 60 minutes, followed by incubation at 80°C for 20 minutes. SBE reactions were performed as follows: 200 nM 5' biotinylated primer (5'→3') CAGCACCTCC[L]TGAGCGTCC (photolinker [L]), 6.25 mM MgCl<sub>2</sub>, 125  $\mu$ M ddNTPs, and 1 unit of Thermipol polymerase (Solis Biodyne, Tartu, Estonia). Reactions were cycled 44 times at 94°C for 10 s, 55°C for 30 s and 72°C for 10 s. SBE products were streptavidin purified with the Genostrep 384 Kit (Bruker Daltonics, Bremen, Germany) and UV cleaved following the manufacturer's protocol. Each sample was measured four times as the average of five spectra on an Autoflex MALDI-TOF mass spectrometer (Bruker Daltonics, Bremen, Germany). Each spectrum was the accumulation of 50 laser shots. Spectral mass results were analyzed with the GenoTools 2.0 software (Bruker Daltonics, Bremen, Germany) and manually checked. The expected mass for unincorporated primer was 2797.78 Daltons, 3082.97 Daltons for the ancestral A allele (an incorporated T), and 3067.96 Daltons for the derived G allele (an incorporated C). A representative spectral graph is shown in Figure S2.

**Researcher Genotyping** DNA was extracted from blood drops taken from the archaeologists, palaeontologists and laboratory researchers involved in the extraction and analysis of the Neanderthal remains using the Chelex method. The *mc1r* gene fragment was

amplified with primers L846-H936, and both strands were directly sequenced on an Applied Biosystems 3700 sequencer (ABI, Foster City, CA, USA). None of the researchers differed at this position and all had the A allele.

**Generating expression vectors** The full-length human *mc1r* open reading frame (accession number NP\_002386) was inserted into the mammalian expression vector pcDps and epitope-tagged with an N-terminal hemagglutinin (HA) epitope and C-terminal Flag epitope by a PCR-based overlapping fragment mutagenesis approach. *Mc1r* mutations were introduced into the tagged version of *mc1r* with a PCR-based site-directed mutagenesis and restriction fragment replacement strategy. For generating stably transfected cells, the double tagged *mc1r* variants (cloned into pcDps) were transferred into pcDNA5™ FRT (Invitrogen, Karlsruhe, Germany). The identity of the various constructs and the accuracy of all PCR-derived sequences were confirmed by restriction analysis and sequencing.

**Generating stable cell lines** We applied the Flp-In System (Invitrogen, Karlsruhe, Germany), which is designed to generate stable mammalian expression cell lines with a single expression cassette, with a *Saccharomyces cerevisiae*-derived DNA recombination system. CHO-K1 cells were stably transfected to express the wild-type and Arg307Gly variant of the huMC1R. Stable cell lines were tested by PCR and a sandwich ELISA (*S15*) for gene integration and protein expression, respectively. Although the system is designed for singular gene integration at identical genomic positions, we tested three clones of each receptor variant using a cAMP accumulation assay to confirm their identical behavior. In brief, a recombinase is deployed for site-specific singular integration of a selected gene into the genome of mammalian cells. Upon co-transfection, the recombinase expressed from a plasmid mediates a homologous recombination between the recombination sites (integrated into the genome of the modified CHO-K1 cells, used in this study) such that *mc1r* (cloned with flanking recombination sites) is inserted into the CHO-K1. Insertion into the genome activates a hygromycin resistance gene, and inactivates the Zeocin (Invitrogen, Karlsruhe, Germany) resistance gene. Thus, stable expression was selected by hygromycin resistance. Furthermore, stable cell lines were tested by PCR and a sandwich ELISA (*S15*) for gene integration and protein expression, respectively. Although the system is designed for singular gene integration at identical genomic positions, we tested three clones of each receptor variant using a cAMP accumulation assay to confirm their identical behavior. Since the clones of each variant yielded similar results (Table S2) and to minimize the risk of differences in the genetic background of the clones, both the three wild-type and the three Arg307Gly clones, were pooled separately and used for further experiments.

**Cell Culture and transfection** COS-7 cells were cultivated in Dulbecco's modified Eagle's medium supplemented with 10% fetal bovine serum, 100 U/mL penicillin, and 100 µg/mL streptomycin at 37°C in a humidified 7% CO<sub>2</sub> incubator. Stably transfected CHO-K1 cells were maintained in Ham's F12 medium supplemented with 10% fetal bovine serum, 100 U/mL penicillin, and 500 µg/mL hygromycin B at 37°C in a humidified 5% CO<sub>2</sub> incubator. Lipofectamine 2000 (Invitrogen, Karlsruhe, Germany) was used for transfecting cells according to the manufacturer's instruction.

**ALPHAScreen cAMP assay** The cAMP content of cell extracts was determined by a non-radioactive cAMP assay based on the ALPHAScreen technology (Perkin Elmer, Waltham, MA, USA) (*S16*). Thus, cells were split into 50 mL cell culture flasks (1 x 10<sup>6</sup> cells/flask) and transfected with a total amount of 5 µg plasmid. One day after transfection, cells were seeded

in 48-well plates ( $5 \times 10^4$  cells/well). One day later, cAMP accumulation assays were performed. Cells were washed once and incubated in serum-free DMEM containing 1 mM 3-isobutyl-1-methylxanthine (Sigma, Munich, Germany) in the absence or in increasing amounts of agonists (NDP- $\alpha$ -MSH or  $\alpha$ -MSH methylxanthine (Sigma, Munich, Germany)), for 1 h at 37°C. The reactions were terminated by aspirating media, and cells were lysed in 50  $\mu$ l lysis buffer (see ALPHAScreen manual) containing 1 mM 3-isobutyl-1-methylxanthine. From each well 5  $\mu$ l of lysate were transferred to a 384-well plate. Acceptor beads (in stimulation buffer without 3-isobutyl-1-methylxanthine) and donor beads were added according to the manufacturer's protocol. Cyclic AMP accumulation data were analyzed by the GraphPad Prism program (version 4.00 for Windows, San Diego, CA, USA).

**[<sup>125</sup>I]-NDP- $\alpha$ -MSH displacement studies** Cells were treated and seeded as described above (ALPHAScreen cAMP assay). Intact cells were assayed 48 h after transfection in competition binding assays using [<sup>125</sup>I]-NDP- $\alpha$ -MSH (100 pM, specific activity 2,000 Ci/mmol, Amersham, Freiburg, Germany) as a tracer. Displacement was performed in 200  $\mu$ l binding buffer (50 mM Hepes (pH 7.2); 5 mM MgCl<sub>2</sub>, 1 mM CaCl<sub>2</sub>, and 0.1% bovine serum albumin) for 3 h at 25°C in a concentration-dependent manner by unlabeled  $\alpha$ -MSH (without, 10 pM, 32 pM, 100 pM, 320 pM, 1 nM, 3.2 nM, 10 nM, 32 nM, 100 nM, 320 nM, 1  $\mu$ M and 3.2  $\mu$ M). Radioligand specifically bound to the receptor was determined after three washing steps (washing buffer: binding buffer with 0.5 M NaCl) and lysis (lysis buffer: 8 mM urea, 2% Nonidet P-40 in 3 M acetic acid). K<sub>i</sub> and B<sub>max</sub> values were calculated from displacement curves with Cheng and Prusoff's method (S17).

**ELISAs** To estimate the amounts of receptor proteins expressed at the cell surface and in all cellular compartments ligand-independently, an indirect cell surface ELISA and a total cellular ELISA, respectively, were used (S18). In brief, to estimate cell surface expression of receptors carrying an amino-terminal HA-tag, transfected cells were seeded into 48-well plates (COS-7) and 24-well plates (CHO), fixed with 4% paraformaldehyde without disrupting the cell membrane, and incubated with a peroxidase-coupled monoclonal anti-HA antibody (3F10; Roche, Grenzach-Wyhlen, Germany). Bound anti-HA antibody was then detected by adding H<sub>2</sub>O<sub>2</sub> and *o*-phenylenediamine (2.5 mM each in 0.1 M phosphate-citrate buffer; pH 5.0) as substrate and chromogen, respectively. After 15 min at room temperature, the enzyme reaction was stopped by adding 1 M HCl containing 0.05 M Na<sub>2</sub>SO<sub>3</sub>, and color development was measured bichromatically at 492 and 620 nm.

For total cellular ELISA, COS-7 or CHO cells were harvested 2 days after transfection (4  $\mu$ g plasmid DNA/60-mm dish) and solubilized in 150  $\mu$ l solubilization buffer (10 mM Tris-HCl (pH 7.4), 150 mM NaCl, 1 mM dithiothreitol, 1 mM EDTA, 1% deoxycholate, 1% Nonidet P-40, 0.2 mM phenylmethylsulfonylfluoride, and 10  $\mu$ g/mL aprotinin) at 4°C for 12 h. Cell debris was removed by centrifugation, and supernatants were used for ELISAs. Microtiter plates were coated (at 4°C for 16 h) with a monoclonal antibody directed against the carboxyl-terminal Flag-tag (Sigma, Munich, Germany). After blocking (with 10% FBS in PBS), cell lysates were applied and incubated at 37°C for 2 h. Plates were washed three times with PBS containing 0.05% TritonX-100 (PBS-T).

Thereafter, a peroxidase coupled anti-HA antibody (3F10; Roche, Grenzach-Wyhlen, Germany) was added, and plates were incubated at 21°C for 2 h. Then, plates were washed with PBS-T three times and H<sub>2</sub>O<sub>2</sub> and *o*-phenylenediamine (2.5 mM each in 0.1 M phosphate-citrate buffer; pH 5.0) were added to serve as substrate and chromogen, respectively. After 15 min at room temperature, the enzyme reaction was stopped by adding 1

M HCl containing 0.05 M Na<sub>2</sub>SO<sub>3</sub>, and color development was measured bichromatically at 492 and 620 nm.

**Immunofluorescence studies** were carried out to examine the subcellular distribution of the MC1R variants. COS-7 cells were transferred into six-well plates containing sterilized glass coverslips and transfected. For immunofluorescence staining cells were fixed with 4% paraformaldehyde 48 h after transfection, permeabilized with 0.05% Triton X-100 in PBS (PBS-T), and incubated with a monoclonal anti-HA antibody (10 µg 12CA5 in PBS-T; Roche, Grenzach-Wyhlen, Germany). The primary mouse antibody was detected using an anti-mouse-IgG TRITC-labeled secondary antibody (Sigma, Munich, Germany). Fluorescence images were obtained with a confocal laser-scanning microscope (LSM 510; Carl Zeiss Jena, Jena, Germany).

**Functional characterization of MC1R variants** To investigate the relevance of Arg307Gly substitution an in-depth functional characterization was performed. First, both variants, wild-type (accession number NM\_002386) and Arg307Gly, were heterologously expressed in COS-7 cells. Because MC1R mediates its signal via Gs/adenylyl cyclase activation, agonist-induced intracellular cAMP levels were determined. As shown in Fig. 1B and Table S2, the wild-type human MC1R responds to the natural agonist  $\alpha$ -MSH with a ~4-fold increase in intracellular cAMP levels. In contrast, Arg307Gly displays significant reductions in basal (40% of the wild-type) and agonist-induced (50% of the wild-type) cAMP formation ( $p < 0.05$ ). EC<sub>50</sub> values are not different between the wild-type MC1R and Arg307Gly. As shown in Fig S3A, elevated basal cAMP levels of the wild-type MC1R strongly correlated with the amount of transfected DNA whereas basal cAMP levels of Arg307Gly showed almost no elevation with increasing amounts of transfected plasmid. The differences in basal and agonist-induced cAMP levels between the wild-type and Arg307Gly variant did not change when cells were serum-starved for 18 h prior to the assays (Fig. S3B).

To exclude the possibility that these differences are due to overexpression in COS-7 cells, we established stable cell lines where a single expression cassette of either MC1R variant was introduced by homologous recombination at a predefined locus (see above). These stably transfected CHO cells also revealed a significant reduction of agonist-induced cAMP levels in the Arg307Gly variant compared to the wild-type (Table S2).

The reduced basal and agonist-induced cAMP levels suggest either lower cell surface expression levels and/or a reduced coupling efficiency of Arg307Gly. To discriminate between the two mechanistic explanations, we determined MC1R protein expression levels in all cellular compartments (total cellular ELISA) performed with cell lysate and at the plasma membrane using a cell surface ELISA and <sup>125</sup>I-NDP- $\alpha$ -MSH binding assay, both performed on intact cells. Although total receptor protein expression did not differ between the two variants in transiently and stably transfected cells (Table S2), radioligand binding studies revealed 47% and 78% reduction of agonist binding sites on the surfaces of COS-7 and CHO cells, respectively, expressing Arg307Gly. No changes were found in K<sub>d</sub> values, illustrating the unchanged ability of the ligand to bind to the receptor (Table S2). Similarly, cell surface expression of the Arg307Gly variant was significantly reduced when ligand-binding was measured independently with the cell surface ELISA (Table S2). The reduction in cell surface expression detected using different methods in combination with the lack of differences in total receptor protein expression suggests a partial intracellular retention of the Arg307Gly variant. Therefore, we performed confocal immunofluorescence studies with transfected COS-7 but found no significant qualitative differences in the subcellular receptor distribution (Fig. S4). In concert with these finding, Western blot studies revealed no

differences in the specific band pattern of the receptor protein (due to glycosylation or receptor multimerization, data not shown) indicating that trafficking deficiency is only partial. In sum, dysfunction of Arg307Gly can not only be attributed to lower cell surface expression levels of the receptor. Rather, it appears that G protein-coupling efficacy is also affected by this substitution (see also below).

Partial loss-of function, as found for Arg307Gly, has been associated with pale skin colour and red hair in humans. However, different mutations appear to impair signalling and hence pigmentation to varying degrees (*S19*). Therefore, we tested human MC1R alleles with low (Val60Leu) and higher (Arg142His, Arg151Cys, Arg160Trp, Asp294His) penetrance (i.e. the proportion of individuals with a certain genotype showing the associated phenotype) in our functional cAMP assay. We confirmed partial activity of the chosen variants, indistinguishable from that of Arg307Gly (Table S2).

Among mammalian MC1R the position corresponding to Arg307 is relatively constant and studies suggest functional intolerance of this position to substitutions (*S20*). In some species, for example in fox (acc. No.: CAH10741), cow (acc. No. AAL38171), and sheep (acc. No.: ABF71418), Arg307 is substituted by Lys and in mouse, by Met (acc. No.: NP\_032585). The functional importance of these species variations is not clear. Therefore, we tested Arg307Lys and Arg307Met substitutions in the human MC1R. As shown in Fig. S5, Arg307Met was essentially like the human wild-type. In contrast, Arg307Lys displayed basal and stimulated cAMP levels significantly higher as the human MC1R wild-type. However, total and cell surface expression levels were similar to the wild-type human MC1R. Our data therefore support the notion that position 307 participates in modulation of G protein-coupling efficiency.

# Supplementary Figures

TCTTCAAGAACTTCAACCTCTTTCTCGCCCTCATCTGCAATGCCATCATCGACCCCTCATCTACGCCCTCCACAGCCAGGAGCTCCGCAGGACGCTCAAGGAGGTGCTGACATGC  
TCCTGGTGA

B.1.1 .....G.....  
B.1.2 .....G.....  
B.1.3 .....T.....  
B.1.4 .....  
B.1.5 .....  
B.1.6 .....  
B.1.7 .....  
B.1.8 .....  
B.1.9 .....  
B.1.10 .....  
B.1.11 .....  
B.1.12 .....  
B.1.13 .....  
B.1.14 .....  
B.1.15 .....  
B.1.16 .....  
B.1.17 .....  
B.1.18 .....  
B.1.19 .....  
B.1.20 .....  
B.1.21 .....  
B.1.22 .....  
B.1.23 .....  
B.1.24 .....  
B.1.25 .....

Monti Lessini (L906-H924)

TCATCTACGCCCTCCACAGCCAGGAGCTCCGCAGGACGCTCAAGGAGGTGCTGACAT

B.2.1 .....G.....  
B.2.2 .....G.....  
B.2.3 .....G.....  
B.2.4 .....  
B.2.5 .....  
B.2.6 .....  
B.2.7 .....  
B.2.8 .....  
B.2.9 .....  
B.2.10 .....  
B.2.11 .....  
B.2.12 .....

Monti Lessini (L884-H936)

TGCAATGCCATCATCGACCCCTCATCTACGCCCTCCACAGCCAGGAGCTCCGCAGGACGCTCAAGGAGGTGCTGACATG

CTCCTGGTGA  
F.1.1 .....G.....  
F.1.2 .....G.....  
F.1.3 .....G.....  
F.1.4 .....G.....  
F.1.5 .....G.....  
F.1.6 .....C.....  
F.1.7 .....C.....  
F.1.8 .....  
F.1.9 .....  
F.1.10 .....  
F.1.11 .....  
F.1.12 .....  
F.1.13 .....  
F.1.14 .....  
F.1.15 .....  
F.1.16 .....  
F.1.17 .....  
F.1.18 .....  
F.1.19 .....  
F.1.20 .....  
F.1.21 .....  
F.1.22 .....  
F.1.23 .....  
F.1.24 .....  
F.1.25 .....  
F.1.26 .....  
F.1.27 .....  
F.1.28 .....  
F.1.29 .....  
F.1.30 .....  
F.1.31 .....  
F.1.32 .....  
F.1.33 .....  
F.1.34 .....  
F.1.35 .....  
F.1.36 .....  
F.1.37 .....  
F.1.38 .....  
F.1.39 .....  
F.1.40 .....  
F.1.41 .....  
F.1.42 .....  
F.1.43 .....



L.3.9  
L.3.10  
L.3.11  
L.3.12  
L.3.13  
L.3.14  
L.3.15  
L.3.16  
L.3.17  
L.3.18

.....  
.....  
.....  
.....  
.....  
.....  
.....  
.....  
.....  
.....

El Sidrón (L906-H924)

B.1.1  
B.1.2  
B.1.3  
B.1.4  
B.1.5  
B.1.6  
B.1.7  
B.1.8  
B.1.9  
B.1.10  
B.1.11  
B.1.12  
B.1.13  
B.1.14  
B.1.15

TCATCTACGCCTTCCACAGCCAGGAGCTCCGCAGGACGCTCAAGGAGGTGCTGACAT

.....G.....  
.....G.....  
.....  
.....  
.....  
.....  
.....  
.....  
.....  
.....  
.....  
.....  
.....  
.....  
.....

El Sidrón (L906-H924)

B.2.1  
B.2.2  
B.2.3  
B.2.4  
B.2.5  
B.2.6  
B.2.7  
B.2.8  
B.2.9  
B.2.10

TCATCTACGCCTTCCACAGCCAGGAGCTCCGCAGGACGCTCAAGGAGGTGCTGACAT

.....G.....  
.....  
.....  
.....  
.....  
.....  
.....  
.....  
.....  
.....  
.....  
.....  
.....  
.....  
.....

El Sidrón (L906-H924)

B.3.1  
B.3.2  
B.3.3  
B.3.4  
B.3.5  
B.3.6  
B.3.7  
B.3.8  
B.3.9  
B.3.10  
B.3.11  
B.3.12  
B.3.13  
B.3.14  
B.3.15  
B.3.16  
B.3.17  
B.3.18  
B.3.19  
B.3.20

TCATCTACGCCTTCCACAGCCAGGAGCTCCGCAGGACGCTCAAGGAGGTGCTGACAT

.....G.....  
.....G.....  
.....G.....  
.....G.....  
.....  
.....  
.....  
.....  
.....  
.....  
.....  
.....  
.....  
.....  
.....  
.....  
.....  
.....  
.....  
.....  
.....

El Sidrón (L906-H924)

B.4.1  
B.4.2  
B.4.3  
B.4.4  
B.4.5  
B.4.6  
B.4.7  
B.4.8  
B.4.9  
B.4.10  
B.4.11  
B.4.12  
B.4.13  
B.4.14

TCATCTACGCCTTCCACAGCCAGGAGCTCCGCAGGACGCTCAAGGAGGTGCTGACAT

.....G.....  
.....  
.....  
.....  
.....  
.....  
.....  
.....  
.....  
.....  
.....  
.....  
.....  
.....  
.....  
.....  
.....  
.....  
.....  
.....  
.....

El Sidrón (L911-H924a)

L.1.1  
L.1.2  
L.1.3  
L.1.4  
L.1.5  
L.1.6

CGCCTTCCACAGCCAGGAGCTCCGCAGGACGCTCAAGGAGGTGCTGACRTG

.....T.....  
.....T.....  
.....  
.....  
.....  
.....

L.1.7	.....
L.1.8	.....
L.1.9	.....
L.1.10	.....
L.1.11	.....
L.1.12	.....
L.1.13	.....
L.1.14	.....
L.1.15	.....
L.1.16	.....
E1 Sidrón (L911-H924a)	CGCCTTCCACAGCCAGGAGCTCCGCAAGGAGGTGCTGACRTG
L.2.1	.....A.....
L.2.2	.....
L.2.3	.....
L.2.4	.....
L.2.5	.....
L.2.6	.....
L.2.7	.....
L.2.8	.....
L.2.9	.....
L.2.10	.....
L.2.11	.....
L.2.12	.....
L.2.13	.....
L.2.14	.....
L.2.15	.....
L.2.16	.....
L.2.17	.....
L.2.18	.....
L.2.19	.....
L.2.20	.....
L.2.21	.....
L.2.22	.....
L.2.23	.....
L.2.24	.....
L.2.25	.....
L.2.26	.....
L.2.27	.....
L.2.28	.....
L.2.29	.....
L.2.30	.....
L.2.31	.....
L.2.32	.....
L.2.33	.....
L.2.34	.....
L.2.35	.....
L.2.36	.....
L.2.37	.....
L.2.38	.....
L.2.39	.....
L.2.40	.....
L.2.41	.....
L.2.42	.....
L.2.43	.....
L.2.44	.....
L.2.45	.....
L.2.46	.....
L.2.47	.....
L.2.48	.....
L.2.49	.....
L.2.50	.....
L.2.51	.....
L.2.52	.....
L.2.53	.....
L.2.54	.....
L.2.55	.....
L.2.56	.....
L.2.57	.....
L.2.58	.....

**Figure S1.** Clone sequences for the different Neanderthal samples and *mc1r* fragments retrieved (first character corresponds to the laboratory, B: Barcelona, F: Florence, L: Leipzig; first digit to number of PCR; second digit to number of clone). The position of the Arg307Gly substitution is indicated in red.

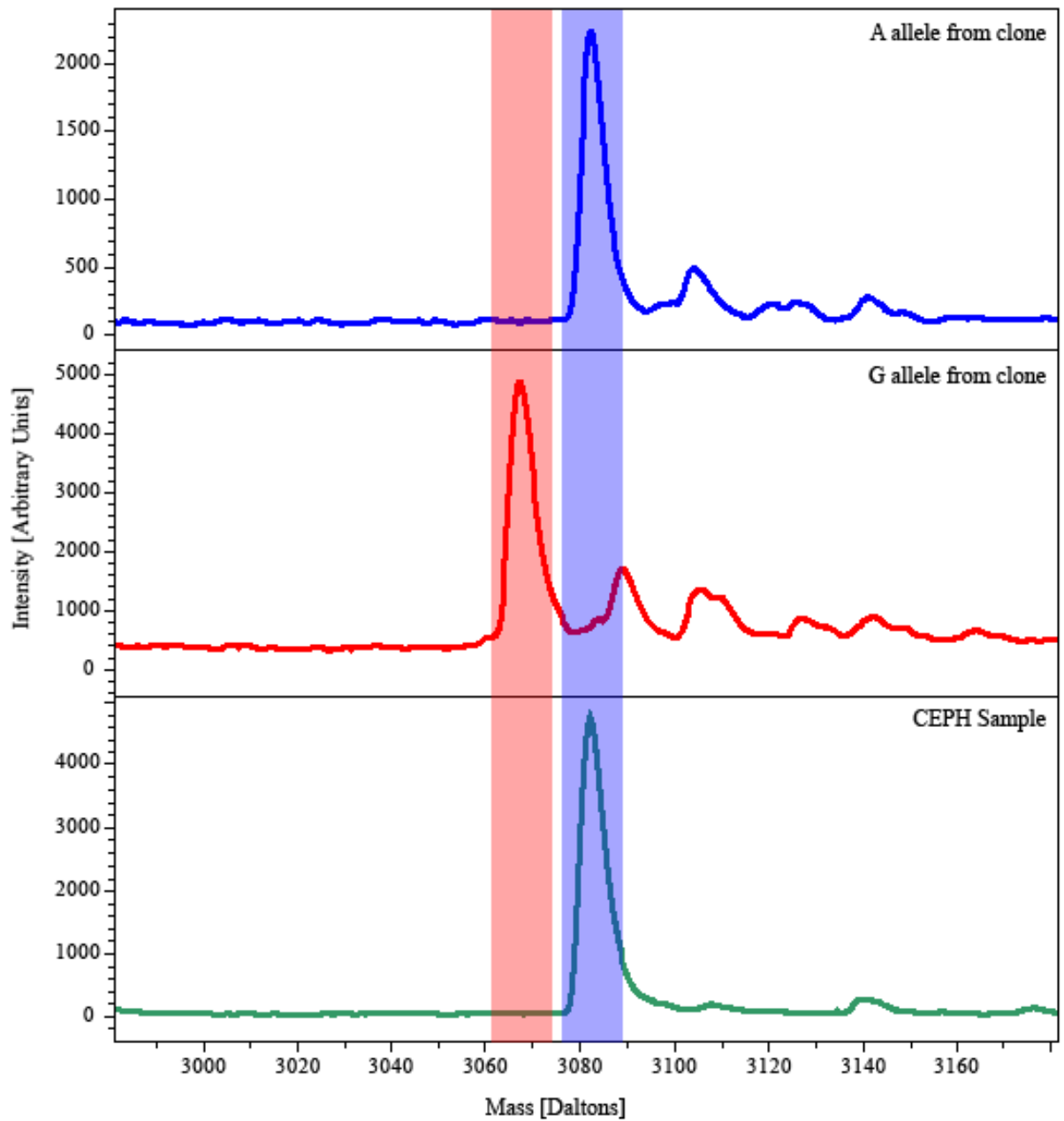


**Figure S2.** Mass spec screening for Arg307Gly variant in the CEPH panel. Mass spectral graph of the A allele control clone (3082.97 Daltons), G allele control clone (3067.96 Daltons) and of a random CEPH sample. All CEPH samples have a homozygous A allele profile similar to the one shown above.

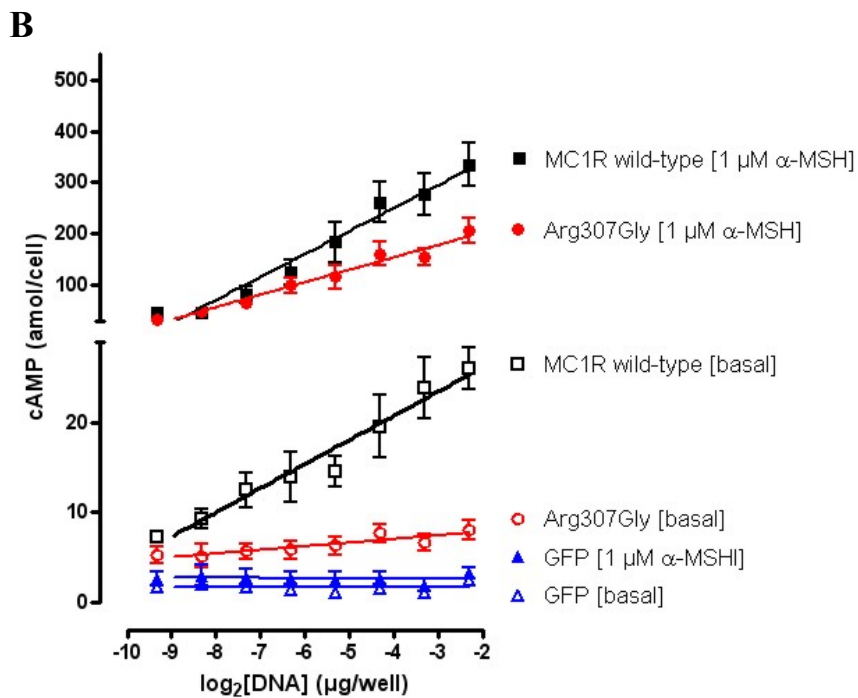
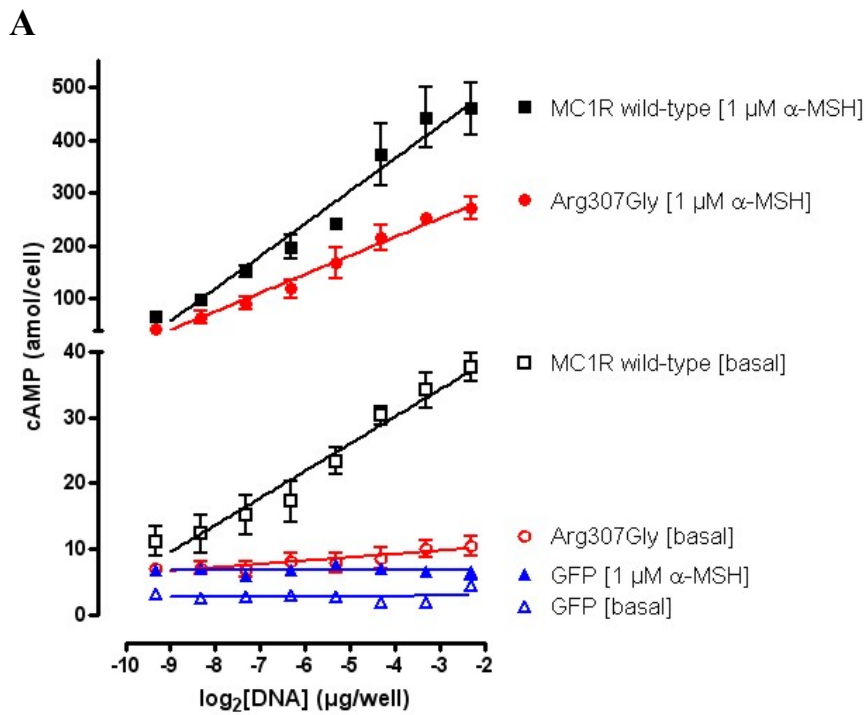


**Figure S3.** Correlation of basal and stimulated receptor activity with the amount of transfected plasmid DNA. COS-7 cells were transfected with increasing amounts of the indicated plasmid DNA. Intracellular cAMP levels were determined 48 h after transfection in the absence (basal) and presence (1  $\mu\text{M}$ ) of  $\alpha$ -MSH. Data are means  $\pm$  S.E.M. of two independent assays, each performed in duplicate.

A) Measurements for cells under normal cultivation conditions. B) Measurements for cells that were starved in serum-free medium 18 h prior to the assay.

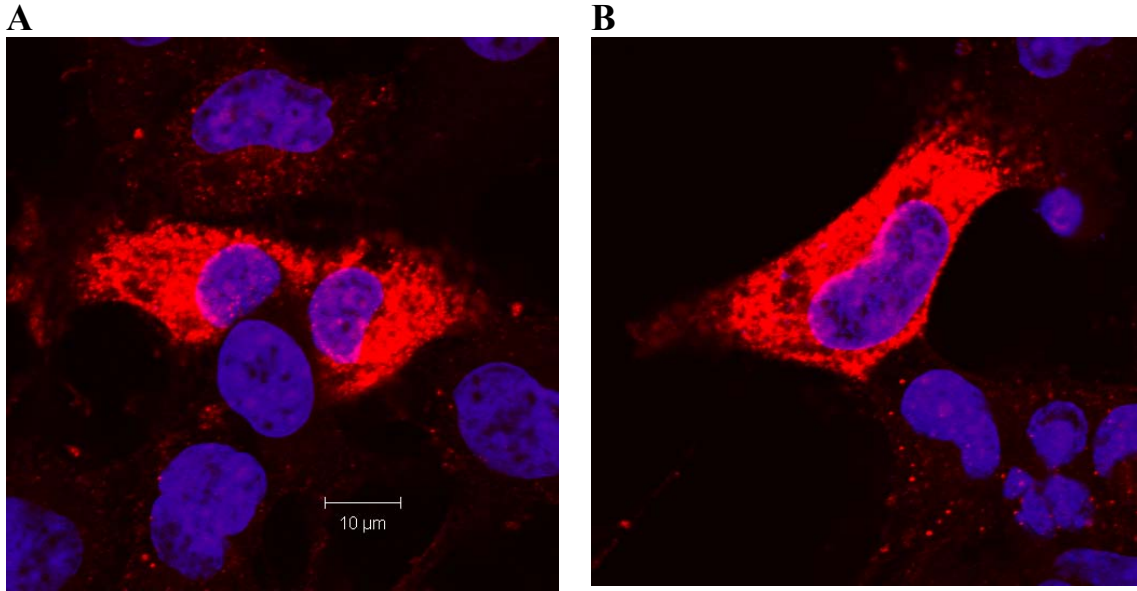


**Figure S4.** Subcellular distribution of the wild type Arg307 (**A**) and Gly307 (**B**) MC1R variants. COS-7 cells were transiently transfected with plasmids encoding the wild-type MC1R and the Gly307 variant of the MC1R. Cells were fixed and permeabilized and HA-tagged receptors were detected with an anti-HA monoclonal antibody and a TRITC-labeled anti-mouse antibody. Pictures of specific fluorescence of HA-tagged GPCR (red) and DAPI-stained nucleus (blue) were taken with a confocal microscope (LSM 510, Zeiss). The pictures shown are representative of two additional independent experiments.

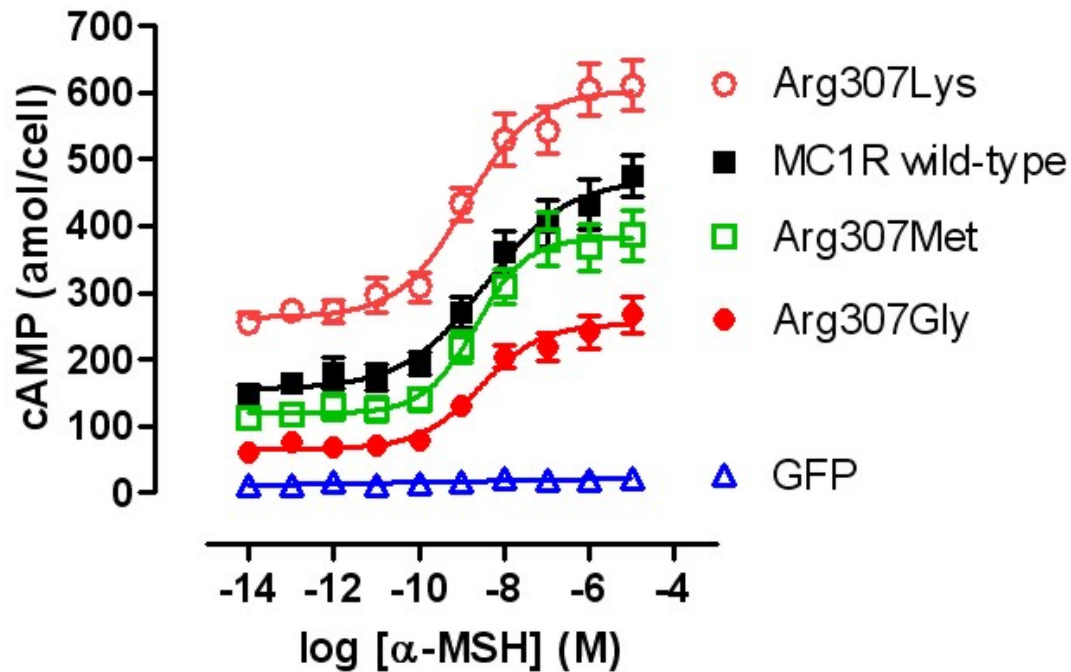


**Figure S5.** Functional characterization of naturally occurring variants at position 307. Comparison of mammalian MC1R orthologs revealed that the position corresponding to Arg307 in human MC1R is substituted by Met in the mouse and Lys in the cow, sheep and fox orthologs. To test for potential functional consequences, these substitutions were introduced into the human MC1R. COS-7 cells transfected with the wild-type human MC1R, the mutants Arg307Lys and Arg307Met and the control (green fluorescent protein) were incubated with increasing concentrations of  $\alpha$ -MSH. Intracellular cAMP levels were determined with the AlphaScreen cAMP assay (see Materials and Methods). Data are means  $\pm$  S.E.M. of four independent assays, each performed in quadruplicate.

## Supplementary Tables

**Table S1. Results for *mc1r* amplification from the two Neanderthal samples.** “A” represents the number of clones carrying an adenine at position 919, “G” the number of clones carrying a guanine,  $\Sigma$  refers to the total number of clones sequenced for an amplicon and %G represents the percentage of clones with a G. The column “lab” designates the laboratory in which the amplifications were done; B: Barcelona, L: Leipzig, F: Florence.

<b>Amplicon</b> (used primer combination)	<b>A</b>	<b>G</b>	<b><math>\Sigma</math></b>	<b>% G</b>	<b>1<sup>st</sup> or 2<sup>nd</sup> extract</b>	<b>lab</b>
Monti Lessini (L846-H936)	24	1	25	4	1 <sup>st</sup>	B
Monti Lessini (L906-H924)	9	3	12	25	1 <sup>st</sup>	B
Monti Lessini (L884-H936)	63	5	68	7	1 <sup>st</sup>	F
Monti Lessini (L911-H924a)	22	0	22	0	1 <sup>st</sup>	L
Monti Lessini (L911-H924a)	18	10	28	36	1 <sup>st</sup>	L
Monti Lessini (L911-H924a)	17	1	18	6	1 <sup>st</sup>	L
El Sidrón (L906-H924)	13	2	15	13	1 <sup>st</sup>	B
El Sidrón (L906-H924)	9	1	10	10	1 <sup>st</sup>	B
El Sidrón (L906-H924)	16	4	20	20	1 <sup>st</sup>	B
El Sidrón (L906-H924)	13	1	14	7	1 <sup>st</sup>	B
El Sidrón (L911-H924a)	16	0	16	0	2 <sup>nd</sup>	L
El Sidrón (L911-H924a)	58	0	58	0	2 <sup>nd</sup>	L

**Table S2. Functional characterization of huMC1R variants and the Arg307Gly variant in cAMP accumulation assay.** To study the functional relevance of the Arg307Gly variant found in two Neanderthals, COS-7 cells were transfected with expression vectors coding for wild-type receptor, Neanderthal variant and various human MC1R mutants known to have an impaired receptor function (See materials and methods for details). Since the clones of each variant yielded similar results and to minimize the risk of differences in the genetic background of the clones, both the three wild-type and the three Arg307Gly clones were pooled separately and used for further experiments. Cells were tested in cAMP accumulation assays. Basal cAMP,  $E_{max}$  and  $EC_{50}$  values were determined from concentration-response-curves (1 fM – 10  $\mu$ M) of two agonists,  $\alpha$ -MSH and NDP- $\alpha$ -MSH, with GraphPad Prism (version 4.00 for Windows, San Diego, CA, USA). Basal cAMP and  $E_{max}$  values are given as x-fold over basal cAMP accumulation of wild-type receptor (basal cAMP in  $\alpha$ -MSH assays: COS-7:  $42.1 \pm 7.1$  amol/cell and CHO-K1:  $16.7 \pm 0.3$  amol/cell; basal cAMP in NDP- $\alpha$ -MSH assays: COS-7:  $38.0 \pm 5.0$  amol/cell). Data are presented as means  $\pm$  S.E.M. of independent experiments (number indicated in parentheses), each carried out in duplicate. Numbers in bold indicate a significant mean value difference between variant and wild-type ( $P < 0.05$ ; two tailed, paired Student t-Test).

MC1R variant	$\alpha$ -MSH			NDP- $\alpha$ -MSH		
	Basal cAMP (fold over wt MC1R basal)	$E_{max}$	$EC_{50}$ (nmol/L)	Basal cAMP (fold over wt MC1R basal)	$E_{max}$	$EC_{50}$ (nmol/L)
<b>COS-7 cells</b>						
wild-type (wt)	1 (14)	$3.6 \pm 0.4$ (14)	$1.4 \pm 0.2$ (14)	1 (11)	$5.2 \pm 0.9$ (11)	$0.4 \pm 0.1$ (11)
Arg307Gly	<b><math>0.4 \pm 0.04</math></b> (13)	<b><math>1.8 \pm 0.2</math></b> (13)	$2.0 \pm 0.6$ (13)	<b><math>0.5 \pm 0.08</math></b> (11)	<b><math>2.6 \pm 0.3</math></b> (11)	$0.3 \pm 0.1$ (11)
Val60Leu	<b><math>0.4 \pm 0.04</math></b> (7)	<b><math>1.2 \pm 0.2</math></b> (7)	$2.0 \pm 0.6$ (7)	<b><math>0.3 \pm 0.04</math></b> (6)	<b><math>1.9 \pm 0.5</math></b> (6)	$0.2 \pm 0.03$ (6)
Arg142His	$0.8 \pm 0.02$ (3)	<b><math>2.3 \pm 0.2</math></b> (3)	$7.4 \pm 1.9$ (3)	$0.7 \pm 0.01$ (3)	<b><math>1.9 \pm 0.1</math></b> (3)	$5.0 \pm 0.8$ (3)
Arg151Cys	$0.6 \pm 0.2$ (4)	<b><math>2.1 \pm 0.2</math></b> (4)	$9.1 \pm 3.7$ (4)	$0.6 \pm 0.1$ (4)	<b><math>2.5 \pm 0.9</math></b> (4)	$0.5 \pm 0.2$ (4)
Arg160Trp	$0.6 \pm 0.2$ (4)	<b><math>1.9 \pm 0.3</math></b> (4)	$1.3 \pm 0.2$ (4)	$0.5 \pm 0.2$ (4)	<b><math>2.2 \pm 0.4</math></b> (4)	$0.6 \pm 0.1$ (4)
Asp294His	$0.7 \pm 0.3$ (4)	<b><math>1.3 \pm 0.2</math></b> (4)	$6.3 \pm 5.1$ (4)	$0.7 \pm 0.1$ (4)	<b><math>2.2 \pm 0.4</math></b> (4)	$4.0 \pm 1.4$ (4)
<b>CHO-K1 cells</b>						
wild-type clone 1	1 (3)	$5.2 \pm 0.4$ (3)	$2.5 \pm 0.7$ (3)			
wild-type clone 2	1 (3)	$5.2 \pm 0.3$ (3)	$2.1 \pm 0.4$ (3)			
wild-type clone 3	1 (3)	$4.6 \pm 0.1$ (3)	$2.5 \pm 0.3$ (3)			
Arg307Gly clone 1	<b><math>0.7 \pm 0.1</math></b> (3)	<b><math>2.3 \pm 0.2</math></b> (3)	$2.4 \pm 0.9$ (3)			
Arg307Gly clone 2	<b><math>0.7 \pm 0.1</math></b> (3)	<b><math>2.4 \pm 0.1</math></b> (3)	$2.5 \pm 0.01$ (3)			
Arg307Gly clone 3	<b><math>0.6 \pm 0.02</math></b> (3)	<b><math>2.3 \pm 0.1</math></b> (3)	$2.5 \pm 0.8$ (3)			
wild-type clone 1-3	1 (7)	$11.6 \pm 2.5$ (7)	$2.2 \pm 0.2$ (7)			
Arg307Gly clone 1-3	<b><math>0.8 \pm 0.1</math></b> (7)	<b><math>4.8 \pm 6.1</math></b> (7)	$2.6 \pm 0.2$ (7)			

**Table S3. Expression and binding properties of wild-type MC1R and the Arg307Gly variant.** For functional characterization, COS-7 cells were transiently and CHO-K1 stably transfected with MC1R wild-type and Arg307Gly construct. Total cellular expression levels (intracellular plus plasma membrane expression) were measured by a sandwich ELISA. Specific optical density (OD) readings (OD value of HA-tagged construct minus OD value of control-transfected cells) are given as a percentage of wild-type HA-tagged human MC1R. The non-specific OD<sub>492 nm</sub> values of control (GFP) -transfected cells COS-7 cells and CHO-K1 cells were  $0.259 \pm 0.023$  and  $0.099 \pm 0.010$  (set 0%), respectively. The specific OD<sub>492 nm</sub> values of the wild-type HA-tagged MC1R in COS-7 cells and CHO-K1 cells were  $1.353 \pm 0.365$  and  $0.220 \pm 0.015$  (set 100%), respectively. Cell surface expression levels (plasma membrane expression) were measured by an indirect cellular ELISA. Specific OD readings (OD value of HA-tagged construct minus OD value of control-transfected cells) are given as a percentage of wild-type HA-tagged human MC1R. The non-specific OD<sub>492 nm</sub> values of control-transfected COS-7 cells and CHO-K1 cells were  $0.030 \pm 0.007$  and  $0.115 \pm 0.019$  (set 0%), respectively. The specific OD<sub>492 nm</sub> values of the wild-type HA-tagged MC1R in COS-7 cells and CHO-K1 cells were  $1.491 \pm 0.056$  and  $0.468 \pm 0.036$  (set 100%), respectively. Binding studies revealed 47% and 78% reduction of agonist binding sites ( $B_{max}$ ) per COS-7 cell and CHO cell, respectively. The affinity for  $\alpha$ -MSH did not significantly differ between the two variants. Data are presented as means  $\pm$  S.E.M. of independent experiments. The number of independent experiments, each carried out in quadruplicate (ELISAs) or duplicates (displacement binding), is given in parentheses. Numbers in bold indicate a significant mean value difference between Arg307Gly and wild-type ( $P < 0.05$ ; two tailed, paired Student t-Test).

MC1R variant	ELISA		<sup>125</sup> I]-NDP- $\alpha$ -MSH	
	Total (% of wt MC1R)	cell surface (% of wt MC1R)	cell surface $B_{max}$ ( $10^3$ receptors/cell)	displacement $K_i$ (nmol/L) competitor: $\alpha$ -MSH
<b>COS-7 cells</b>				
wild-type (wt)	100 (6)	100 (4)	$53.0 \pm 5.4$ (3)	$1.1 \pm 0.2$ (3)
Arg307Gly	$106 \pm 3$ (6)	<b><math>86.6 \pm 0.7</math> (4)</b>	<b><math>28.2 \pm 2.2</math> (3)</b>	$1.3 \pm 0.1$ (3)
<b>CHO-K1 cells</b>				
wild-type (wt)	100 (9)	100 (9)	$8.7 \pm 0.2$ (3)	$2.8 \pm 0.2$ (3)
Arg307Gly	$100 \pm 3$ (9)	<b><math>44.9 \pm 4.4</math> (9)</b>	<b><math>1.9 \pm 0.1</math> (3)</b>	$4.2 \pm 0.5$ (3)

**Table S4.** BLASTN 45 most similar hits for the MC1R positions 846-936 fragment with the putative Neanderthal variant. Max scores for the environmental database are 38.2 (query coverage of 21%).

Description	Max. Score	Max. identity
Homo sapiens MC1R	168	98%
Pan troglodytes MC1R	168	98%
Gorilla gorilla MC1R	168	98%
Pongo pygmaeus	161	97%
Mandrillus sphinx	153	96%
Papio hamadryas	153	96%
Papio anubis	153	96%
Macaca mulatta	153	96%
Macaca nigra	153	96%
Macaca silvana	153	96%
Cercopithecus neglectus	153	96%
Presbytis comata	145	95%
Colobus gereza	145	95%
Macaca silenus	145	95%
Macaca nemestrina	145	95%
Cercopithecus mitis	145	95%
Cercopithecus diana	145	95%
Cercopithecus aethiops	145	95%
Miopithecus talapoin	145	95%
Allenopithecus nigroviridis	145	95%
Hylobates concolor	145	95%
Trachypithecus francoisi	137	94%
Trachypithecus obscurus	137	94%
Trachypithecus cristatus	137	94%
Trachypithecus auratus	137	94%
Semnopithecus entellus	137	94%
Erythrocebus patas	129	93%
Saimiri oerstedii	129	93%
Saguinus midas	129	93%
Saguinus oedipus	129	93%
Saguinus geoffroyi	129	93%
Saguinus imperator	129	93%
Hylobates muelleri	129	95%
Hylobates lar	129	95%
Eulemur fulvus	125	93%
Saguinus fuscicollis	121	92%
Callimico goeldii	121	92%
Callithrix jacchus	121	92%
Callithrix geoffroyi	121	92%
Callithrix argentata	121	92%
Callithrix pygmaea	121	92%
Leontopithecus chrysomelas	121	92%
Varecia variegata	117	92%
Cebus albifrons	115	92%

### Supplementary references

- S1. S. Condemni, *Éditions du Comité des Travaux Historiques et Scientifiques* (2001).
- S2. C. Corrain, *Memorie del Museo di Scienze Naturali di Verona* **16**, 97 (1968).
- S3. A. Rosas *et al.*, *PNAS* **103**, 19266 (December 19, 2006, 2006).
- S4. J. Fortea *et al.*, *Estudios Geológicos* **59**, 157 (2003).
- S5. D. Caramelli *et al.*, *Current Biology* **16**, R630 (2006).
- S6. C. Lalueza-Fox *et al.*, *Current Biology* **16**, R629 (2006).
- S7. D. Caramelli *et al.*, *PNAS* **100**, 6593 (May 27, 2003, 2003).
- S8. N. Rohland, M. Hofreiter, *Biotechniques* **42**, 343 (2007).
- S9. M. T. P. Gilbert, H.-J. Bandelt, M. Hofreiter, I. Barnes, *Trends in Ecology & Evolution* **20**, 541 (2005).
- S10. H. Römpler *et al.*, *Nat. Protocols* **1**, 720 (2006).
- S11. A. W. Briggs *et al.*, *Proc Natl Acad Sci U S A* **104**, 14616 (Sep 11, 2007).
- S12. P. Brotherton *et al.*, *Nucleic Acids Res* (Aug 22, 2007).
- S13. J. Sambrook, D. W. Russell, *3rd Edition 3rd Edition* (2001).
- S14. H. M. Cann *et al.*, *Science* **296**, 261b (April 12, 2002, 2002).
- S15. H. Römpler *et al.*, *Science* **313**, 62 (July 7, 2006, 2006).
- S16. K. Sangkuhl, H. Römpler, W. Busch, B. Karges, T. Schöneberg, *Human Mutation* **25**, 505 (2005).
- S17. Y. Cheng, W. Prusoff, *Biochem Pharmacol.* **22**, 3099 (1973).
- S18. T. Schöneberg, V. Sandig, J. Wess, T. Gudermann, G. Schultz, *J. Clin. Invest.* **100**, 1547 (September 15, 1997, 1997).
- S19. J. L. Rees, *Annual Review of Genetics* **37**, 67 (2003).
- S20. P. A. Kanetsky *et al.*, *Cancer Epidemiol Biomarkers Prev* **13**, 808 (May, 2004).